Can an Internal Hydraulic Jump be Inferred from the Depositional Record of a Turbidity Current ?

S.Kostic & G. Parker
National Center for Earth-surface Dynamics, St. Anthony Falls Laboratory, Minneapolis, Minnesota, USA, 55414, kost0067@tc.umn.edu

ABSTRACT: Turbidity currents emanating from a submarine canyon and debouching onto an associated submarine fan often undergo an internal hydraulic jump near the canyon-fan transition. It is hypothesized here that the sudden decline in bed shear stress due to an internal hydraulic jump leaves a clear signature in the sediment deposit. This hypothesis is studied using the numerical model presented below. The experimental data of Garcia (1993) on turbidity currents near a canyon-fan transition are used to verify the model. Numerical experiments with input parameters similar to those of Garcia (1993) are designed in order to demonstrate that under the right conditions turbidity currents mark the resulting sediment deposit in a submarine canyon-fan system by leaving a detectible depositional signature at the location of the jump. The model is then employed to investigate the characteristics of the depositional signature created by a generic field-scale turbidity current.

1 INTRODUCTION

Turbidity currents are a dominant driving mechanism responsible for the genesis of submarine canyons and associated fans. A typical canyon-fan configuration is illustrated in Figure 1 (Pirmez, 1994). It encompasses a) a relatively steep-slope, narrow submarine canyon excavated by net erosive underflows and b) a low-slope, fan-shaped submarine fan or abyssal plain placed by net depositional underflows. Submarine fans are either channelized or unchannelized. Here the case of fans traversed by distinct, well-formed channels is analyzed. The channels act to limit lateral spread of turbidity currents.

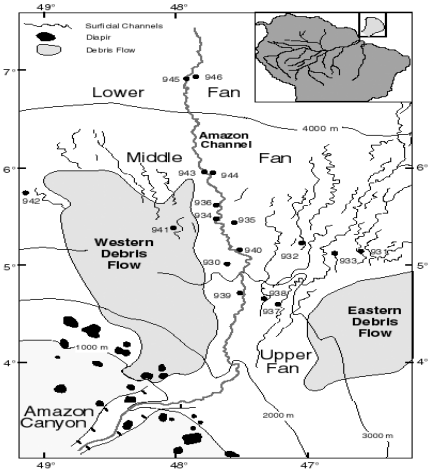

Figure 1. Typical configuration of a submarine canyon-fan system. Amazon Canyon & Fan (from Pirmez, 1994)

Decrease in slope in the downstream direction can cause a turbidity current to undergo an internal hydraulic jump near the canyon-fan transition. A hydraulic jump, internal or otherwise, is a zone of rather sharp transition from a high-velocity supercritical flow upstream to a low-velocity subcritical flow downstream. In open-channel flow, a supercritical regime is described by the standard Froude number greater than a value near unity, while a subcritical regime corresponds to a Froude number less than a value near unity. In turbidity currents, the standard roude number is substituted by the densimetric Froude number.

Generally, supercritical flows exert a relatively high shear stress on the bed, whereas subcritical flows exert a relatively low shear stress on the bed. The sudden decline in bed shear stress due to an internal hydraulic jump might be expected to leave a clear signature in the sediment deposit, e.g. turbidites, created by a turbidity current in the vicinity of a canyon-fan transition.

The nature of the hydraulic jump and the resultant deposits have been the subject of speculation. Menard (1964) related the development of levees bordering deep-sea channels to the thickening of a turbidity current after a hydraulic jump. Van Andel & Komar (1969) interpreted the characteristics of sediment deposits in enclosed basins in terms of the hypothesized occurrence of a hydraulic jump. Mutti (1977) suggested that turbidity currents undergoing a change in slope drop excess sand due to a hydraulic jump, thus causing characteristic turbidites just downstream. Recently, Russell & Arnott (2003)

provided stratigraphic evidence of hydraulic jump conditions in a subaqueous glaciolacustrine fan succession in the Oak Ridges Moraine, southern Ontario, Canada (Figure 2).

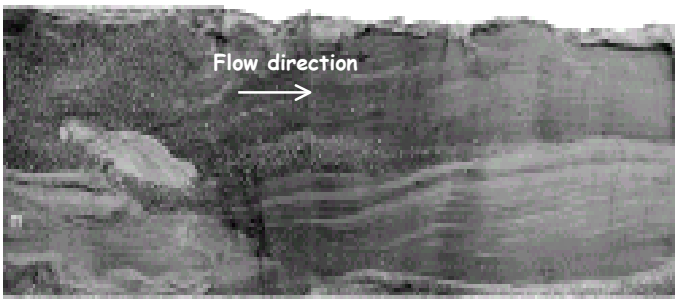

Figure 2. Depositional signature left by a hydraulic jump. The Oak Ridge Moraine, Canada (from Russell & Arnott, 2003)

Internal hydraulic jumps in sediment-driven flows remain unobserved in the field. As for observation at experimental scale, only a few studies are available (Garcia, 1989, 1993; Lamb et al., 2004; Toniolo, 2003). Garcia & Parker (1989) and Garcia (1993) induced a hydraulic jump at a sharp change in slope, Lamb et al. (2004) and Toniolo (2003) created a hydraulic jump by ponding the turbidity current downstream.

The goal of the work reported here is to demonstrate how a numerical model can be employed to investigate whether a hydraulic jump can be really inferred from the depositional record. The experimental data of Garcia (1993) are used for calibration and verification of the numerical model. The model is applied to various scenarios of turbidity currents developing along a sloping bed at experimental scale. A field-scale simulation provides insight into the characteristics of a depositional signature resulting from a generic field-scale turbidity current.

2 MODEL FORMULATION

2.1 *Geometric set-up*

The numerical model presented herein is intended to simulate turbidity currents of constant width propagating along the bed of a canyon-fan system. The model allows for a bed of arbitrary geometry. However, in the numerical simulation at experimental and field scale shown bellow the initial bed profile is assumed to consist of an upstream portion with constant, positive slope joining continuously to a downstream portion that is horizontal. This bed configuration is illustrated in Figure 3. The sloping upstream portion represents a loose surrogate for a submarine canyon, and the horizontal downstream portion is a loose surrogate for a submarine fan or abyssal plain.

2.2 *Governing equations*

A dense bottom underflow propagating along a canyon-fan system can be described by the following set of single-layer, layer-averaged equations in dimensionless form:

$$\frac{\partial \hat{h}}{\partial \hat{t}} + \frac{\partial \hat{U}\hat{h}}{\partial \hat{x}} = \frac{0.00153\hat{U}}{0.0204 + \frac{1}{Frd_0^2}\frac{\hat{C}\hat{h}}{\hat{U}^2}} \tag{1}$$

$$\frac{\partial \hat{U}\hat{h}}{\partial \hat{t}} + \frac{\partial \hat{U}^2\hat{h}}{\partial \hat{x}} = -\frac{1}{2Frd_0^2}\frac{\partial \hat{C}\,\hat{h}^2}{\partial \hat{x}} - \frac{\hat{C}\,\hat{h}}{Frd_0^2}\frac{\partial \hat{\eta}}{\partial \hat{x}} - c_D\,\hat{U}^2 \tag{2}$$

$$\frac{\partial \hat{C}\hat{h}}{\partial \hat{t}} + \frac{\partial \hat{C}\hat{U}\hat{h}}{\partial \hat{x}} = \hat{v}_s\left(\frac{e_s}{C_0} - r_0\,\hat{C}\right) \tag{3}$$

$$(1-\lambda)\frac{\partial \hat{\eta}}{\partial \hat{t}} = \hat{v}_s\left(r_0\,C_0\,\hat{C} - e_s\right) \tag{4}$$

where $\hat{t} = tU_0/h_0$, $\hat{x} = x/h_0$, $\hat{v}_s = v_s/U_0$, $\hat{h} = h/h_0$, $\hat{U} = U/U_0$, $\hat{C} = C/C_0$, $\hat{\eta} = \eta/h_0$, t = time, x = bed-attached downslope distance, h = turbidity current thickness, U = layer-averaged current velocity, C = layer-averaged concentration of suspended sediment, and η = elevation of the bed. h_0 and U_0 are respectively the current thickness and velocity at the canyon head.

The formulation contains the following dimensionless parameters: Frd_0 = densimetric Froude number at the canyon head, c_D = bed friction coefficient, r_0 = an order-one multiplicative constant, C_0 = suspended sediment concentration at the canyon head, e_S = sediment entrainment coefficient, $\hat{v}_s$ = fall velocity of sediment, S_i = initial bed slope, and λ = sediment porosity.

The densimetric Froude number Frd_0 expresses the ratio of inertial to buoyancy force at the canyon head, and is given by

$$Frd_0 = \frac{U_0}{\sqrt{RgC_0h_0}} \tag{5}$$

where g is gravitational acceleration, and R is the submerged specific gravity of the sediment (= 1.65 for quartz silt).

The entrainment of sediment into suspension by turbidity currents is here estimated from the model of Kostic & Parker (2003), which accommodates different formulations for numerical simulations at experimental and at field scale. The model is adapted from the relations by Garcia & Parker (1993), and Wright & Parker (in press). That is, the entrainment coefficient e_s takes the form:

$$e_s = k\frac{aZ^5}{1+\frac{a}{0.3}Z^5} \tag{6}$$

where k is an adjustment coefficient, and a is a constant, given as follows:

$$k = \begin{cases} 1, & \text{exp. scale} \\ 0-0.01, & \text{field scale} \end{cases} \tag{7}$$

$$a = \begin{cases} 1.3\cdot 10^{-7}, \text{Garcia \& Parker (1993)}, & \text{exp. scale} \\ 7.8\cdot 10^{-7}, \text{Wright \& Parker (2003)}, & \text{field scale} \end{cases} \tag{8}$$

The adjustment of k at field scale is not a part of the original relations, but is introduced here to account for limits on the erodibility of the bed over which the turbidity current runs. In addition, Z is a similarity variable, defined as:

$$Z = \alpha_1 \frac{u_*}{v_S} Re_p^{\alpha_2} S_f^{\alpha_3} \tag{9}$$

In the above equation u_* = shear velocity due to skin friction, Re_p = particle Reynolds number, S_f = friction slope, and $\alpha_1, \alpha_2, \alpha_3$ = parameters, given by:

$$u_* = \sqrt{c_D}\, U \tag{10}$$

$$Re_p = \sqrt{RgD}\, D/\nu \tag{11}$$

$$S_f = c_D Frd^2, \quad Frd = U/\sqrt{RgCh} \tag{12}$$

$$(\alpha_1, \alpha_2) = \begin{cases} (0.586, 1.23), & \text{Re}_p \le 2.36 \\ (1.0 \quad , 0.6\ ), & \text{Re}_p > 2.36 \end{cases} \tag{13}$$

$$\alpha_3 = \begin{cases} 0, & \text{exp. scale} \\ 0.07, & \text{field scale} \end{cases} \tag{14}$$

with D = median grain size of the sediment, ν = kinematic viscosity of water, and Frd = densimetric Froude number.

Finally, the fall velocity v_S is a function of particle Reynolds number. Here it is calculated from the relation of Dietrich (1982).

The details on the dimensionless analysis can be found in Kostic & Parker (in prep.). It is useful to note from Eqs. (1)-(14) that any characteristic parameter Y of the flow field of an underflow emanating from a submarine canyon and debouching onto an associate fan can be expressed as a function of the following dimensionless parameters:

$$Y = f\left(Frd_0, \text{Re}_p, v_S/U_0,\ u_*/v_S, c_D, r_0, C_0, \lambda, S_i\right) \tag{15}$$

In the work reported here the ratio u_*/v_s is replaced by the bed Shield number τ^* which characterizes the degree to which the flow can mobilize the bed sediment. It is defined as

$$\tau^* = \frac{u_*^2}{gRD} \tag{16}$$

2.3 *Initial and boundary conditions*

Initial and boundary conditions for the numerical model are discussed in detail in Kostic & Parker (in prep.). At t = 0 the dependent dimensionless variables h, U and C at all nodal points are set equal to 1. The initial bed elevation for every grid point is determined from a prescribed initial slope S_i. Because of the hyperbolic nature of governing equations, the number and location of physical boundary conditions correspond to the number and location of characteristics that propagate into the flow domain (Kostic & Parker, 2003a).

For the supercritical inflow boundary considered here, which corresponds to a high-velocity flow near the head of a canyon, three boundary conditions needs to be formulated, that is

$$\hat{h}\left(x=0,t\right)=1,\ \hat{U}\left(x=0,t\right)=1,\ \hat{C}\left(x=0,t\right)=1, \tag{17-19}$$

while the outflow BC's take the form

$$\hat{U}\left(x=s,t\right)=\frac{ds}{dt},\ \hat{\eta}\left(x=s,t\right)=\hat{\eta}_o\left(s\right) \tag{20,21}$$

where η_o is an antecedent bed elevation as yet unmodified by the turbidity current, and s denotes the position of the turbidity current head in a deforming grid.

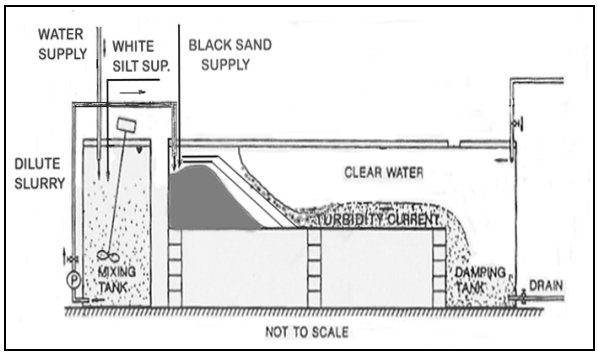

Figure 3. Experimental set-up.

Once an underflow covers the prescribed length of a computational domain, no physical boundary condition is required for either supercritical or subcritical flow unless a downstream control is imposed there. This is indeed the case in the numerical simulations at experimental scale that follow. In the experiments of Garcia & Parker (1989) and Garcia (1993) the condition of a critical densimetric Froude number at the outflow boundary

needs to be imposed to account for a free outfall (Figure 3).

The remaining variables are calculated from the flow domain by means of first-order extrapolation.

2.4 *Numerical scheme*

The governing Eqs. (1-4), together with the initial and boundary conditions, are solved numerically by the explicit ULTIMATE QUICKEST method (Leonard 1979 & 1991), which is third-order in both time and space. The scheme provides a robust, mass-conservative formulation that is capable of dealing with highly advective transport and complex boundary conditions. More comprehensive consideration of the algorithm can be found in Kostic & Parker (2003a).

3 NUMERICAL SIMULATIONS AT EXPERIMENTAL SCALE

3.1 *Validation of the model*

The numerical model is validated using experiments by Garcia (1993) on internal hydraulic jumps in turbidity currents driven by well-sorted sediment. The experimental flume is shown in Figure 3. It was 30 cm wide and 70 cm deep. A submarine canyon was modeled by a 5 m long inclined bed with a slope of 0.08 ($\theta = 4.6^{0}$), followed by a 6.6 m long horizontal bed that represented the associated abyssal plain. A free outfall at the end of the horizontal region acted as a downstream control. The currents were allowed to develop until a quasi-steady state continuous flow was reached.

Table 1. Input parameters for the numerical model

Exp.	h (cm)	U (cm/s)	C x 10^3	D (μm)	Run time (min)
DAPER4	3.0	8.3	2.95	9	33
DAPER7	3.0	8.3	8.60	9	30
GLASSA2	3.0	8.3	3.39	30	30
GLASSA5	3.0	8.3	3.94	30	30
GLASSA7	3.0	11.0	2.66	30	30
GLASSB1	3.0	11.0	3.00	65	38
GLASSB2	3.0	11.0	6.00	65	27
GLASSB3	3.0	11.0	1.50	65	28

As can be seen from Table 1, the inlet current thickness was kept at 3 cm. The corresponding flow rate per unit width was set at either 25 or 33 cm^2/s, yielding inlet velocities of 8.3 and 11.0 cm/s respectively. The median grain size D of the sediment used to generate the turbidity currents was 4, 9, 30 and 65 μm. However, the underflows driven by 4-μm sediment are not of interest for the work presented here, since they were too fine to produce any noticeable deposit in the canyon-fan system during the designed run time. Inlet Reynolds numbers were always larger than 2700, ensuring turbulent conditions there. Additional input parameters include the estimated bed friction coefficient c_D = 0.01 and the estimated sediment porosity $\lambda = 0.5$.

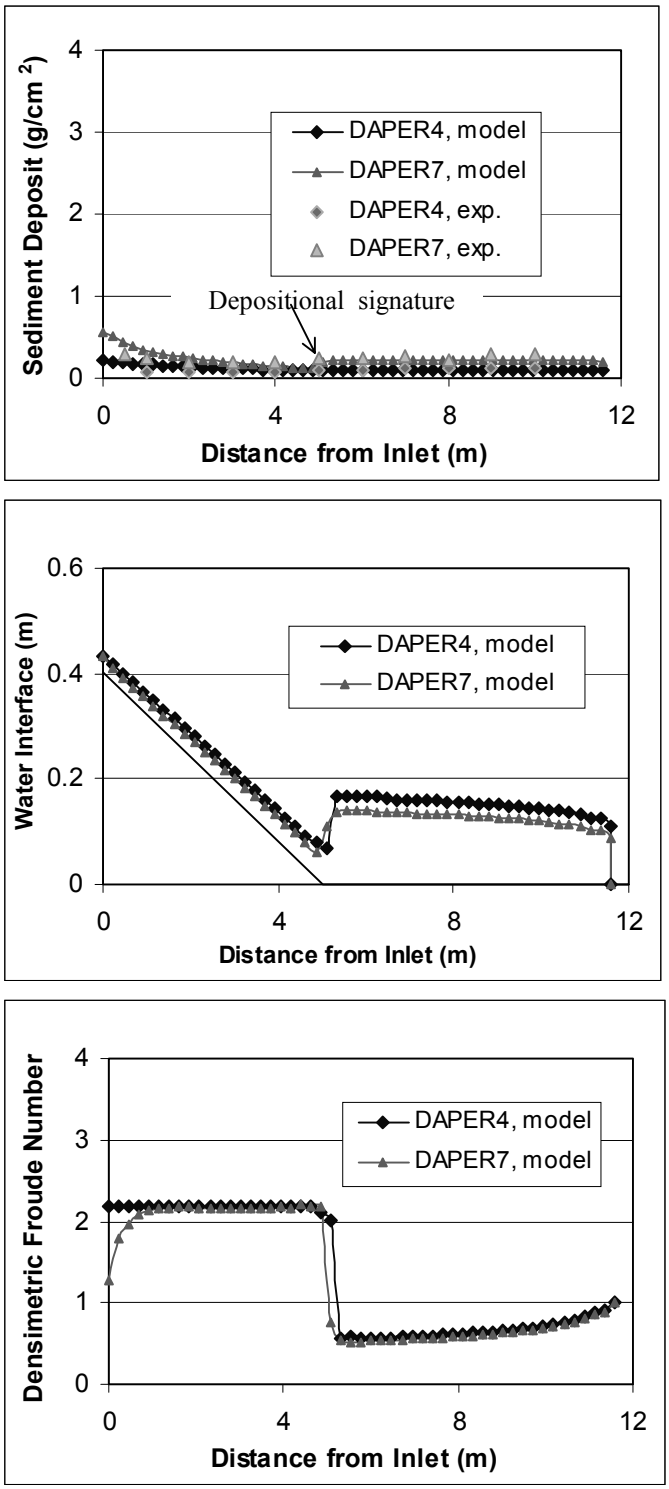

Figure 4. Turbidity current driven by 9-μm sediment: (a) Depositional pattern (b) Underflow interface with an internal hydraulic jump (c) Densimetric Froude number

Figures 4a, 5a and 6a demonstrate good agreement between measured and simulated streamwise variation in sediment mass deposited per unit bed area by turbidity currents driven by 9, 30 and 65 sediment respectively. Both the observations and calculations pertain to the end of each run. The best fit with experimental observations was attained with $r_0 = 1$ for the runs with 9 and 30 μm. For the runs with 65-μm sediment the best fit was obtained with this multiplicative constant set equal to 2. These choices can be loosely justified by the sediment concentration profiles that appear to be more uniform in vertical in underflows driven by fine-grained sediment.

Figures 3b, 4b and 5b show the numerical predictions of the interface elevation $\eta+h$ for turbidity currents driven by 9, 30 and 65 μm respectively, while the Figures 3c, 4c and 5c

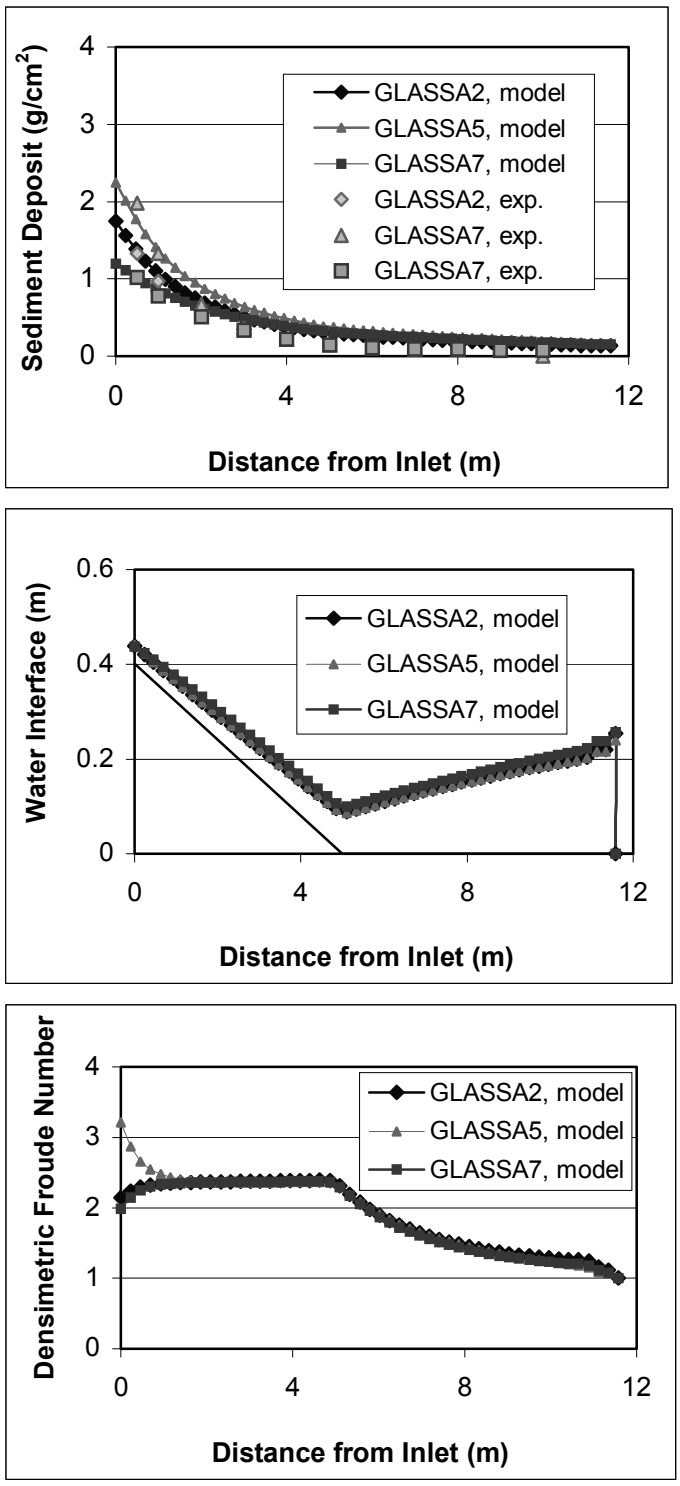

Figure 5. Turbidity current driven by 30-μm sediment: (a) Depositional pattern (b) Water interface with an internal hydraulic jump (c) Densimetric Froude number

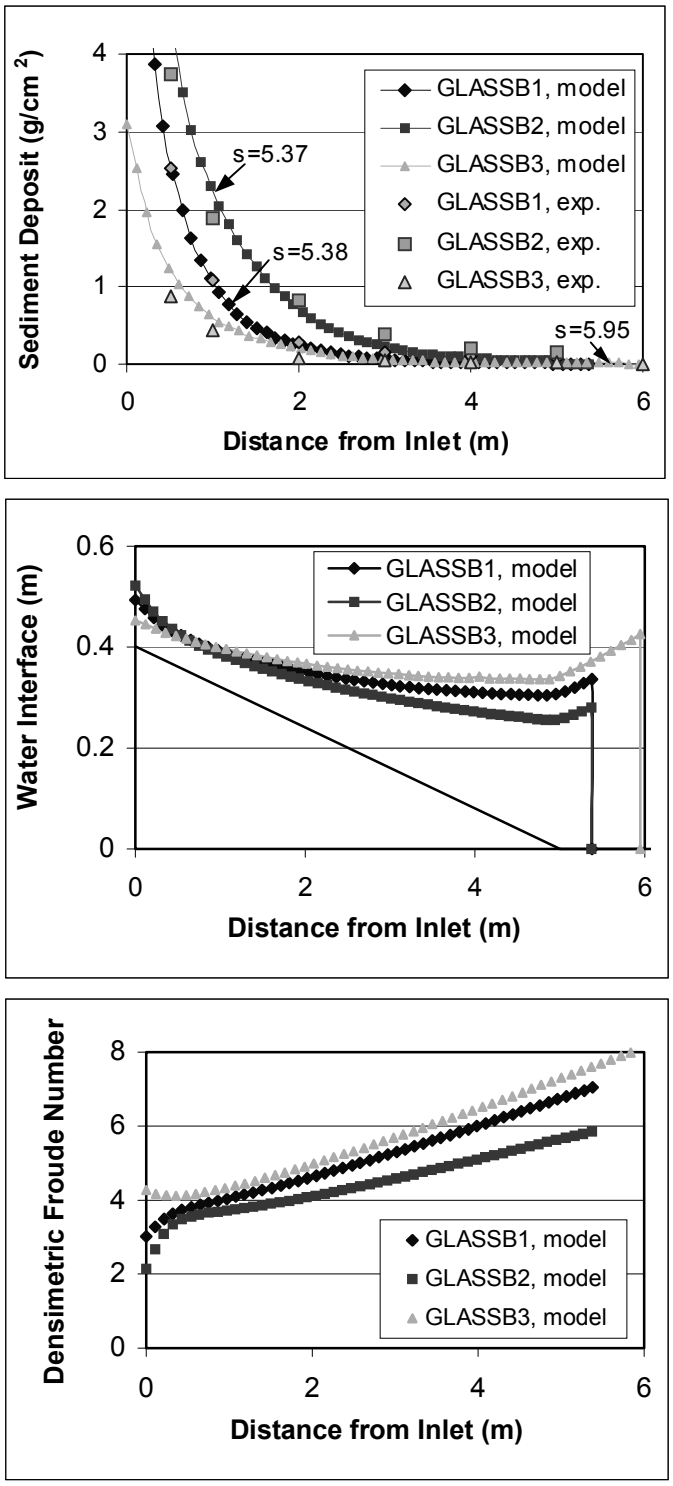

Figure 6. Turbidity current driven by 65-μm sediment: (a) Depositional pattern (b) Water interface with an internal hydraulic jump (c) Densimetric Froude number

illustrate how the corresponding densimetric Froude number *Frd* varies along the model canyon-fan system. Experimental data for the current interface and densimetric Froude number are not available.

The numerical results support experimental observations by Garcia (1993), that can be summarized as follows:

a) Currents driven by 9-μm sediment are weakly depositional along the canyon and fan (Figure 4a). They reach the end of the model fan at x = 11.6 m. They are supercritical along the canyon, and subcritical on the fan, with a distinct intervening hydraulic jump (Figure 4b,c).
b) 30- and 65-μm currents are strongly depositional, and create turbidites that display roughly exponential decrease in thickness with distance from the sediment source (Figure 5a, 6a).
c) 30-μm currents reach the end of model fan, while continuously decelerating and thickening after the slope break (Figure 5b). They do not show evidence of an internal hydraulic jump (Figure 5c).
d) 65-μm currents rapidly disintegrate before they reach the end of the model fan (Figure 6b,c). According to the numerical predictions, they die out when the layer-averaged concentration of suspended sediment drops to below 0.1 % of the inlet value, e.g. at the distance x = 5.38 m for run GLASSB1, x = 5.37 m for run GLASSB2 and x = 5.95 m for run GLASSB3. These flows deposit too rapidly to display an internal hydraulic jump (Figure 6c), a result confirmed by Choi & Garcia (1995).

For the work presented here the most important observation of Garcia (1993) is that the break in canyon-fan slope does not seem to cause any clear discontinuity in the depositional pattern of those currents which are capable of reaching the downstream end of the fan. This notwithstanding, the present numerical simulations of experiments that involved an internal hydraulic jump reveal a modest but clear depositional signature associated with a drop in shear stress right after the jump. This is manifested in terms of an upstream-facing "step" or thickening of the deposit from the upstream to the downstream side of the jump. For example, in the case of runs DAPER4 and DAPER7 the simulated deposit mass per unit bed area shows an increase of 0.0053 and 0.076 g/cm^2 respectively across zone of the jump.

A close inspection of the experimental data of Figures 4a, 5a and 6a reveals that the measurements of run DAPER7 contains such a depositional signature as well (Figure 4a). The step is near the numerically predicted size. In the case of run DAPER 4, the predicted step is sufficiently small that it would not have been clearly seen in the data (Figure 4a). There is no evidence of a depositional signature in the data for the 30- and 65-μm currents, which do not undergo a jump (Figure 5a, 6a). Therefore, the data and numerical results for run DAPER7 provide the first relatively clear hint that under the right conditions a hydraulic jump might leave a depositional signature. This hint is pursued in the numerical experiments below.

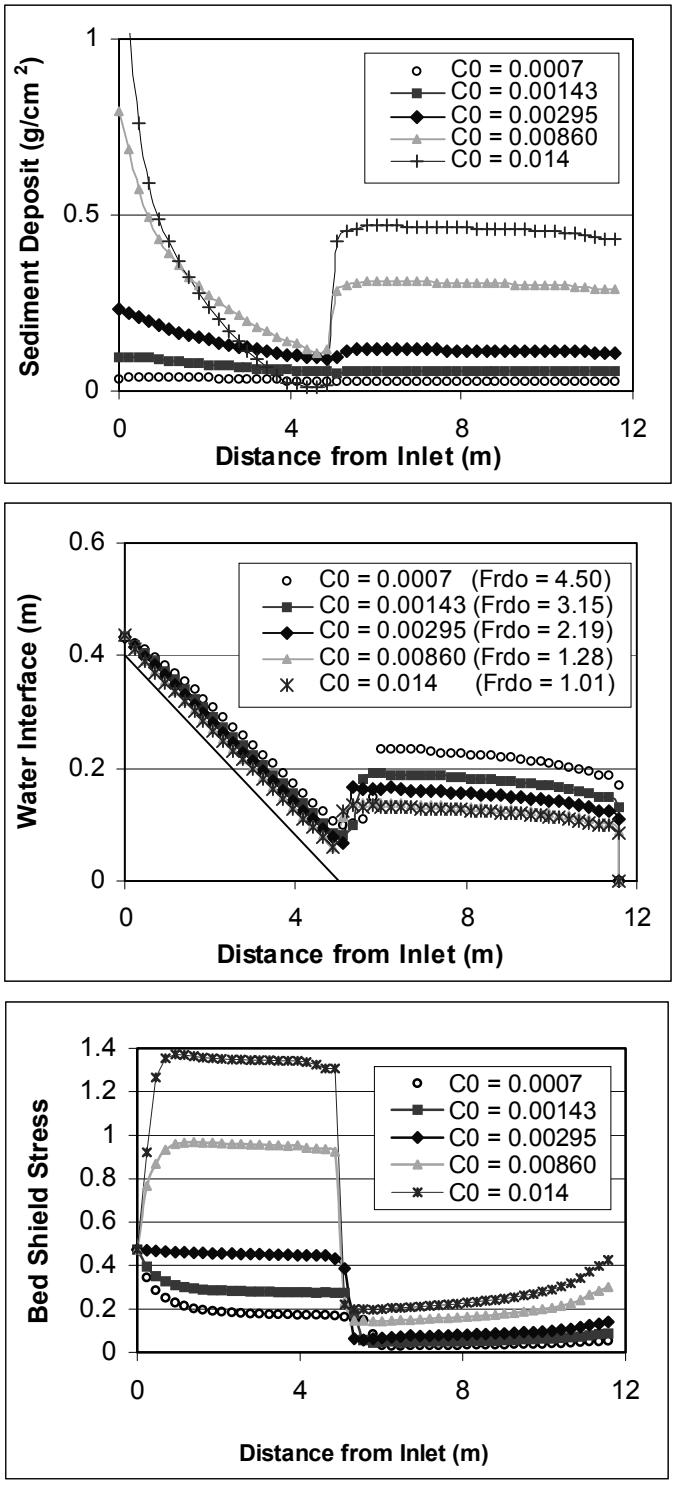

Figure 7. Numerical experiments with 9-μm sediment: (a) Depositional pattern (b) Water interface with an internal hydraulic jump (c) Bed Shield stress

3.2 *Numerical experiments at laboratory scale*

Having found that the numerical model can reproduce the features of turbidity currents near the experimental canyon-fan transition reported by Garcia (1993), the model is now extended to a parametric study of hydraulic jumps. The details on this study can be found in Kostic & Parker (in prep.).

Numerical experiments presented here, however, aim to demonstrate how runs using the DAPER material (9 μm) can under certain conditions can leave a noticeable depositional signature. In particular, the effect of suspended sediment concentration C_0 at the canyon mouth on the formation of an internal hydraulic jump and a corresponding depositional signature is elucidated below.

The model input parameters are: h_0 = 3 cm, U_0 = 8.3 cm/s, R = 1.65, run time = 40 min. The inflow volumetric concentration of suspended sediment is varied in the range $0.0007 \leq C_0 \leq 0.014$. The lower limit is intended to simulate a dilute underflow, and the upper limit is selected to describe an underflow with an inflow densimetric Froude number close to the unity.

Figure 7a reveals that denser turbidity currents tend to deposit sediment from their very inception, and are in general more erosive in the supercritical region, and more depositional in the subcritical region. An increasing drop in shear stress associated with the jump (Figure 7c) is responsible for a successively more pronounced depositional signature (Figure 7a). In addition, turbidity currents with lower inflow buoyancy flux are slower and thicker in both their super- and subcritical regions (Figure 7b), with an internal hydraulic jump that forms farther downstream of the canyon-fan break.

An increased drop in shear stress and consequently more noticeable depositional step can be also obtained by changing some other dimensionless parameters, such as e.g., by increasing the bed resistance c_D, or the initial canyon slope S_i (see Kostic & Parker (in prep.)).

4. MODEL APPLICATION AT FIELD SCALE

It is useful to demonstrate how the numerical model can be employed to investigate the qualitative and quantitative characteristics of a depositional signature at field scale. Therefore, a generic model reach is designed to be representative of a canyon-fan system in the field.

Froude similarity is used to scale-up the input parameters associated with 9 μm material (DAPER) to field dimensions. That is

$$Frd_f = Frd_e \tag{22}$$

where the subscript "f" denotes "field", and the subscript "e" denotes "experiment". Assuming that R is the same in the experiments and the field, (22) results in

$$\frac{(U)_f}{(U)_e} = (\chi_h\ \chi_C)^{1/2} \tag{23}$$

with the scale ratios for length and concentration defined as

$$\chi_h = \frac{(h)_f}{(h)_e} \qquad \chi_C = \frac{(C)_f}{(C)_e} \tag{24}$$

Here the length scale ratio is set to 300, and concentration scale ratio to 1. The field model thus has the following input parameters: h_0 = 9 m, U_0 = 1.4 m/s, C_0 = 0.003, R = 1.65 and c_D = 0.0025. A scale-up of fall velocity in the same way as Eq. (23) results in a grain size D = 20 μm. The canyon-fan system is assumed to be 3.48 km long. The initial bed profile of the system has a break at 1.5 km, such that the bed slope upstream and downstream of the break is 4% and 0%, respectively.

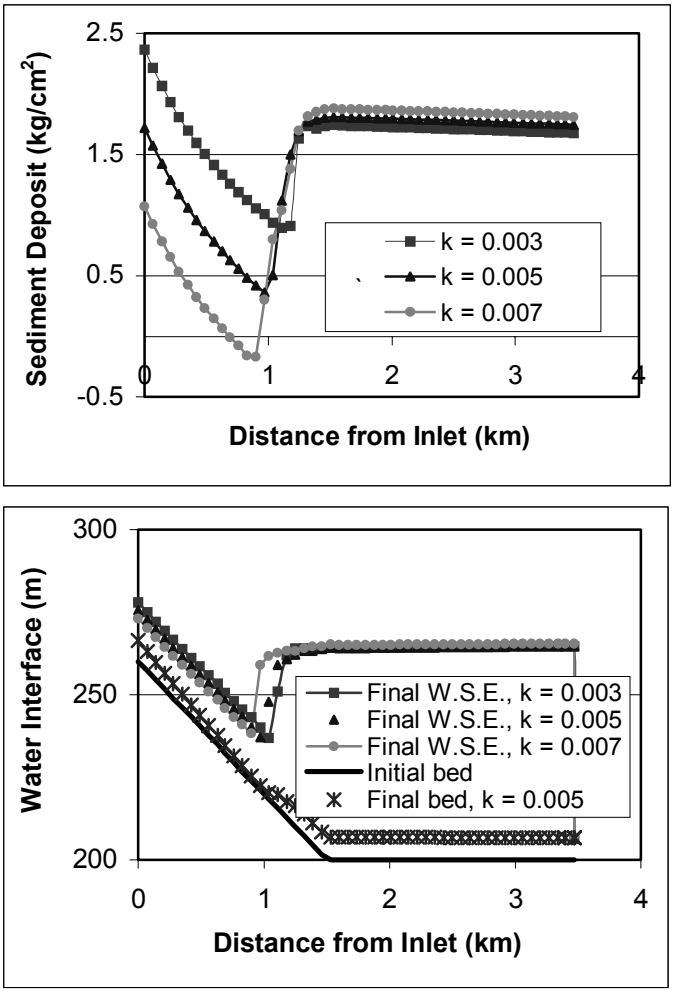

Figure 8. Numerical simulations at field scale: (a) Depositional pattern (b) Current interface and final bed

No downstream control is imposed, so as to allow turbidity currents to propagate freely. Total computation time is 60 days of continuous flow. In the field, this 60 days would be divided into a series of smaller flow durations, e.g. a few hours or days, with long dormant periods in between.

It is value to note here that in the numerical simulations at field scale the adjustment coefficient k of the sediment entrainment model (see Eqs. (6-14)) must be set equal to a value smaller than the unity in order to obtain physically realistic solutions. The adjustment coefficient k may be interpreted as a limitation on the supply of sediment from the bed that is available for entrainment due to e.g. partial consolidation of the bed. In the case when $k = 0$, a purely depositional turbidity current is generated. If however $0.007 < k \leq 1$, a turbidity current accelerates so strongly that the energy constraints of Parker et al. (1986) fail to be satisfied. The end result is a pronounced and unphysical numerical scouring along the entire canyon-fan system.

Therefore, the following values of the adjustment coefficient are set in the calculation: $k = 0.003$, $k = 0.005$ and $k = 0.007$. Figure 8a illustrates that more erosive underflows create far more noticeable depositional signatures at the location of an internal hydraulic jump. Also, the jump is pushed further upstream from the canyon-fan break (Figure 8b). The final bed elevation is presented in Figure 8b for $k = 0.005$. It reveals: a) a clear depositional step associated with the hydraulic jump; b) a change in slope gradient associated with the slope break; and c) a deposit of uniform thickness in the subcritical region.

5 CONCLUSIONS

Results of the numerical model reported here provide clear evidence that turbidity currents can under some circumstances leave a more or less pronounced depositional signature where they go through an internal hydraulic jump driven by declining slope. The depositional signature is created by the sudden drop in bed shear stress generated by the internal hydraulic jump. Therefore, the location of such a depositional signature defines the location of an internal hydraulic jump as well.

The model was successfully verified against the experiments by Garcia (1993) on internal hydraulic jumps in turbidity currents driven by well-sorted sediment. The experimental observations and numerical predictions for Garcia's run DAPER7 provide the first hint that under the right conditions a hydraulic jump might leave a depositional signature. Numerical experiments reveal that a depositional step becomes indeed more noticeable than the one reproduced by the run DAPER7 for higher values of e.g. suspended sediment concentration C_0 at the canyon head, bed resistance c_D or initial canyon slope S_i. Numerical simulations at field scale provide insight into the characteristics of a depositional signature resulting from a generic field-scale turbidity current. It is demonstrated that swifter turbidity currents leave more detectible depositional signatures.

REFERENCES

Dietrich, E. W., 1982, Settling velocity of natural particles, Water Resources Research, 18 (6), 1626-1982.

Choi, S. U. & Garcia, M. 1995. Modeling of one-dimensional turbidity currents with a dissipative – Galerkin finite element method. *J.Hydr.Research*, Vol.33, 623-647.

Garcia, M. & Parker, G., 1989, Experiments on hydraulic jumps in turbidity currents near a canyon-fan transition, *Science*, 245, 393-396.

Garcia, M., 1993, Hydraulic jumps in sediment-driven bottom currents, *Journal of Hydraulic Engineering*, 1993, 1094-1117.

Garcia, M. & Parker, G. 1993. Experiments on the entrainment of the sediment into suspension by a dense bottom current. *J.Geoph. Research*., 98, 4793-4807.

Kostic, S. & Parker, G., in prep. Internal hydraulic jumps created by turbidity currents at slope break – Formation limits and depositional signature.

Kostic, S. & Parker, G., 2003, Progradational sand-mud deltas in lakes and reservoirs: Part 1. Theory and numerical modeling, *Journal of Hydraulic Research*, 41 (2), 127-140.

Lamb, M. P.,Hickson, T., Marr, J. G., Sheets, B., Paola, C. & Parker, G., 2004, Surging versus continuous turbidity currents: flow dynamics and deposits in an experimental intraslope minibasin, *Journal of Sedimentary Research,* 74(1).

Leonard, B.P., 1979, A stable and accurate convection modeling procedure based on quadratic upstream interpolation, *Comp. Methods in Applied Mechanics and Engineering*, 19, 59-98.

Leonard, B.P.,1991, The ULTIMATE conservative difference scheme applied to unsteady one-dimensional advection, *Comp. Methods in Applied Mechanics and Engineering*, 88, 17-77.

Menard, H. W., 1964, *Marine Geology of the Pacific*, McGraw-Hill, New York.

Mutti, E., 1977, Distinctive thin-bedded turbidite facies and related depositional environments in the Eocene Hecho Group (South-central Pyrenees, Spain), *Sedimentology*, 24, 107-131.

Parker, G., Fukushima, Y. & Pantin, M.H., 1986, Self-accelerating turbidity currents, *Journal of Fluid Mechanics*, 171, 145-181.

Pirmez, C., 1994, *Growth of a Submarine Meandering Channel-levee System on the Amazon Fan*, Ph.D. thesis, Columbia University, New York, USA.

Russell, H. A. J. & Arnott, R. W. C., 2003, Hydraulic-jump and hyperconcentrated-flow deposits of a glacigenic subaqueous fan: Oak Ridges Moraine, southern Ontario, Canada, *Journal of Sedimentary Research*, 73(6).

Toniolo, H., 2003, Debris flow and turbidity current deposition in the deep sea and reservoirs, Ph.D. thesis, University of Minnesota, 233 p.

Van Andel, T. H. & Komar, P. D., 1969, Ponded sediment of the Mid-Atlantic Ridge between 22 and 23 degrees north latitude, *Bulletin of Geological Society of America*, 80, 1163-1190.

Wright, S. & Parker, G., in press, Flow resistance and suspended load in sand-bed rivers: simplify stratification model, *Journal of Hydraulic Engineering*.